

Untwisting the Boerdijk-Coxeter Helix

Robert L. Read read.robert@gmail.com

Abstract. The Boerdijk-Coxeter helix (BC helix, or tetrahelix) is a face-to-face stack of regular tetrahedra forming a helical column. Considering the edges of these tetrahedra as structural members, the resulting structure is attractive and inherently rigid, and therefore interesting to architects, mechanical engineers, and robotocists. A formula is developed that matches the visually apparent helices forming the outer rails of the BC helix. This formula is generalized to a formula convenient to designers. Formulae for computing the parameters that give edge-length minimax-optimal tetrahelices are given, defining a continuum of tetrahelices of varying curvature. The endpoints of the optimality of this continuum are the BC helix and a structure of zero curvature, the *equitetrabeam*. Numerically finding the rail angle from the equation for pitch allows optimal tetrahelices of any pitch to be designed. An interactive tool for such design and experimentation is provided: <https://pubinv.github.io/tetrahelix/>. A formula for the inradius of optimal tetrahelices is given. Utility for static and variable geometry truss/space frame design and robotics is discussed.

Key words. Boedijk-Coxeter helix, tetrahelix, robotics, tetrobot, unconventional robots, structural engineering, mechanical engineering, tensegrity, variable-geometry truss

18 AMS subject classifications. 51M15

1. Introduction. The Boerdijk-Coxeter helix[3] (BC helix), is a face-to-face stack of tetrahedra that winds about a straight axis. Because architects, structural engineers, and robotics are inspired by and follow such regular mathematical models but can also build structures and machines of differing or even dynamically changing length, it is useful to develop the mathematics of structures formed from tetrahedra where we relax regularity.

The vertices of the tetrahedra lie upon three helices about the central axis. The Glussbot[11] (or Tetrobot)[8] uses the regularity of this geometry to make a tentacle-like robot that can crawl like a slug or mollusc. These modular robot systems uses mechanical actuators which can change their length, connected by special joints, such as the 3D printable Song-Kwon-Kim[15] joint in the case of the Glussbot, or the CMS joint[7], in the case of the Tetrobot, which allow many members to meet in a single point. Such machines can follow purely regular mathematical models such as the Boerdijk-Coxeter helix or the Octet Truss[4].

31 Buckminster Fuller called the BC helix a *tetrahelix*[5], a term now commonly used. In
 32 this paper we reserve *BC helix* to mean the purely regular structure and use *tetrahelix* to refer
 33 to any structure isomorphic to the BC helix.

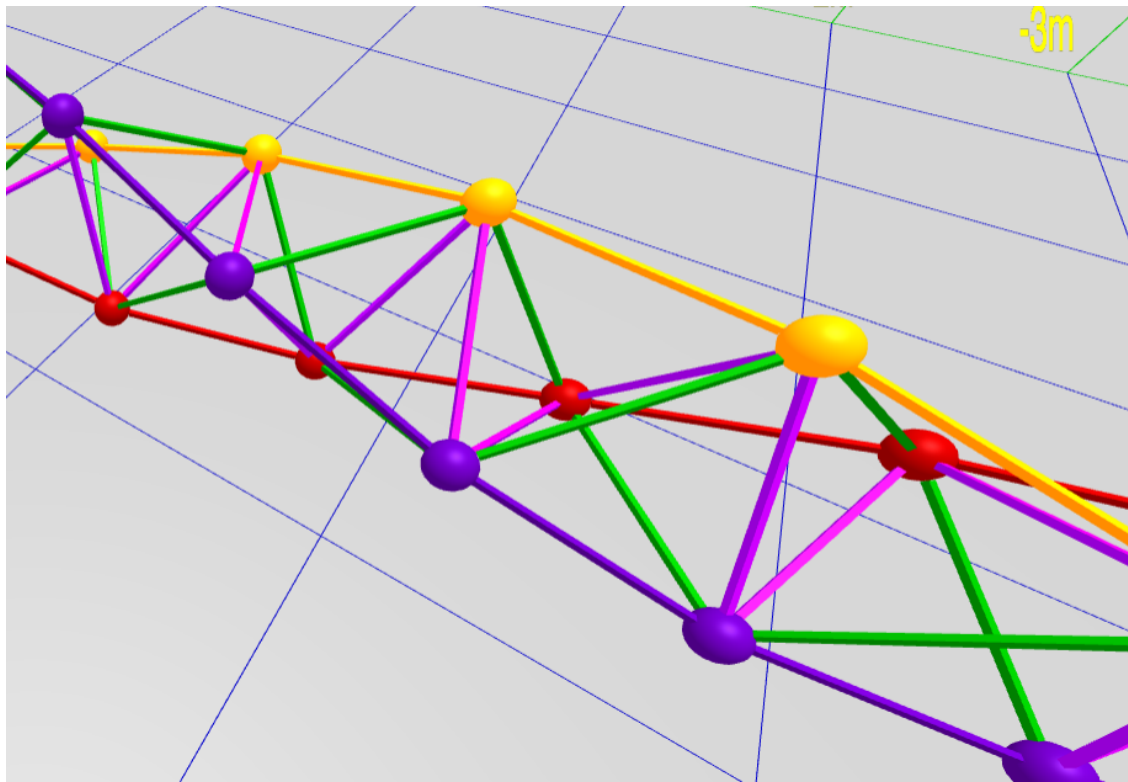


Figure 1. BC Helix Close-up (partly along axis)

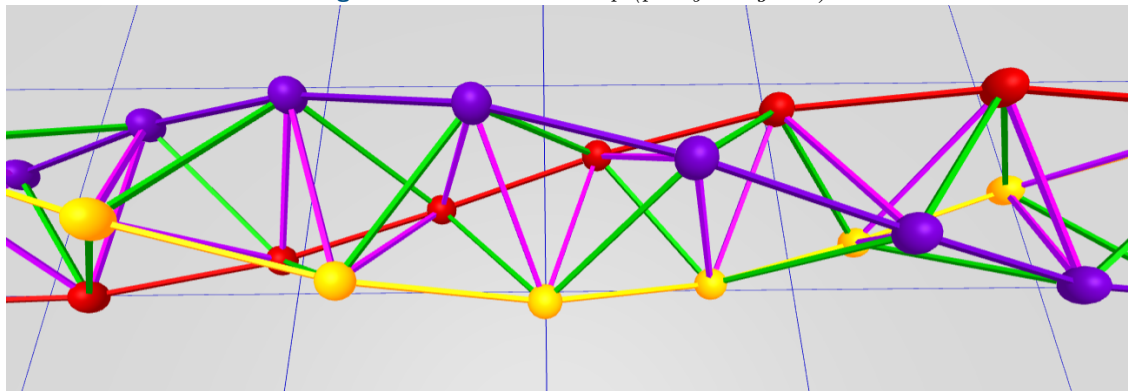


Figure 2. BC Helix Close-up (orthogonal)

34 Imagining Figure 2 as a static mechanical structure, we observe that it is useful to the
 35 mechanical engineer or robotocist because the structure remains an inherently rigid, omni-
 36 triangulated space frame, which is mechanically strong. Imagine further in Figure 2, that each
 37 static edge was replaced with an actuator that could dynamically become shorter or longer in
 38 response to electronic control, and the vertices were a joint that supported sufficient angular
 39 displacement for this to be possible. An example of such a machine is a glussbot, shown in
 40 Figure 12.

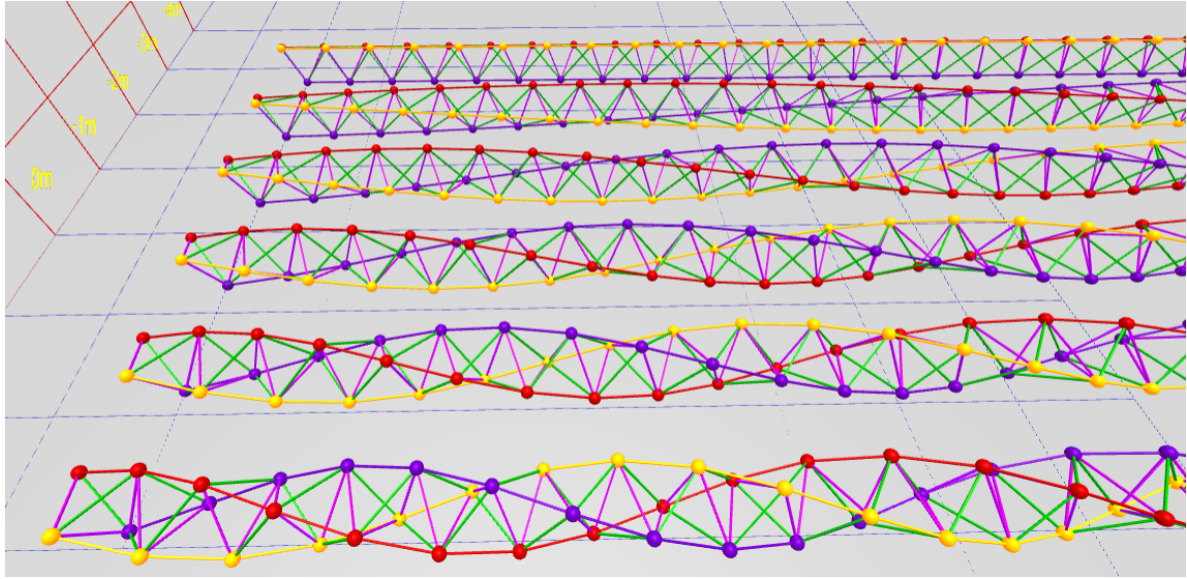


Figure 3. A Continuum of Tetrahelices

41 A BC helix does not rest stably on a plane. It is convenient to be able to “untwist” it and
 42 to form a tetrahelix space frame that has a flat planar surface. By making length changes in a
 43 certain way, we can untwist a tetrahelix to form a *tetrabeam* which has planar faces and has,
 44 for example, an equilateral triangular profile. This paper develops the equations needed to
 45 untwist the tetrahelix. All math developed here is available in JavaScript and demonstrated
 46 by an interactive design website <https://pubinv.github.io/tetrahelix/>[12], from which Figure 2
 47 and the figures below are taken.

48 Figure 3 displays a continuum of tetrahelices optimal in a certain sense, which is the result
 49 of this paper. The closest helix is the BC helix, and the furthest is the equitetrabeam, defined
 50 in section 6.

51 **2. A Designer’s Formulation of the BC Helix.** We would like to design nearly regular
 52 tetrahelices with a formula that gives the vertices in space. Eventually we would like to design
 53 nearly regular tetrahelices by choosing the lengths of a small set of members. In a space frame,
 54 this is a static design choice; in a tetrobot, it is a dynamic choice that can be used to twist
 55 the robot and/or exert linear or angular force on the environment.

56 Ideally we would have a simple formula for defining the nodes based on any curvature
 57 or pitch we choose. It is a goal of this paper to relate these two approaches to generating a
 58 tetrahelix continuum.

59 H.S.M Coxeter constructs the BC helix[3] as a repeated rotation and translation of the
 60 tetrahedra, showing the rotation is:

$$61 \quad \theta_{bc} = \arccos(-2/3)$$

62 and the translation:

$$63 \quad h_{bc} = 1/\sqrt{10}$$

64 θ_{bc} is approximately $0.37 \cdot 2\pi$ radians or 131.81 degrees. The angle θ_{bc} is the rotation of
 65 each tetrahedron, not the tetrahedra along a rail. In [Figure 2](#), each tetrahedron has either a
 66 yellow, blue, or red outer edge or rail. That is, a blue-rail tetrahedron is rotated slightly more
 67 than a 1/3 of a revolution to match the face of the yellow tetrahedra.

68 R.W. Gray's site[\[6\]](#), repeating a formula by Coxeter[\[3\]](#) in more accessible form, gives the

69 Cartesian coordinates $\begin{bmatrix} x \\ y \\ z \end{bmatrix}$ for a counter-clockwise BC Helix in a right-handed coordinate
 70 system:

$$71 \quad (1) \quad \mathbf{V}(n) = \begin{bmatrix} r_{bc} \cos n\theta_{bc} \\ r_{bc} \sin n\theta_{bc} \\ nh_{bc} \end{bmatrix}, \text{ where: } \begin{aligned} r_{bc} &= \frac{3\sqrt{3}}{10} \approx 0.5196 \\ h_{bc} &= 1/\sqrt{10} \approx 0.3162 \\ \theta_{bc} &= \arccos(-2/3) \end{aligned}$$

72 where n represents each integer numbered node in succession on every colored rail.

73 The apparent rotation of a vertex an outer-edge, $\mathbf{V}(n)$ relative from $\mathbf{V}(n+3)$ for any
 74 integer n in [\(1\)](#), is $3\theta_{bc} - 2\pi$.

75 This formula defines a helix, but it is not any of the apparent helices, or *rail* helices, of the
 76 BC helix, but rather one that winds three times as rapidly through all nodes. To a designer of
 77 tetrahelices, it is more natural to think of the three helices which are visually apparent, that
 78 is, those three which are closely approximated by the outer edges or rails of the BC helix. We
 79 think of each of these three rails as being a different color: red, blue, or yellow. This situation
 80 is illustrated in [Figure 4](#), wherein the black helix represents that generated by [\(1\)](#), and the
 81 colored helices are generated by [\(2\)](#).

82 In order to develop the continuum of slightly irregular tetrahelices described in [section 7](#),
 83 we need a formula that gives us the nodes of just one rail helix, denoted by color c and integer
 84 node number n :

$$85 \quad (\forall n \in \mathbb{Z}, \forall c \in \{0, 1, 2\} : \mathbf{H}_{BCcolored}(n, c) = \mathbf{V}(3n + c))$$

86 Such a helix can be written:

$$87 \quad (2) \quad \mathbf{H}_{BCcolored}(n, c) = \begin{bmatrix} r_{bc} \cos ((3\theta_{bc} - 2\pi)n + c\theta_{bc}) \\ r_{bc} \sin ((3\theta_{bc} - 2\pi)n + c\theta_{bc}) \\ 3h_{bc}(n + c/3) \end{bmatrix}, \text{ where } \begin{aligned} r_{bc} &= \frac{3\sqrt{3}}{10} \\ h_{bc} &= 1/\sqrt{10} \\ \theta_{bc} &= \arccos(-2/3) \end{aligned}$$

88 In this formula, integral values of n may be taken as a node number for one rail and
 89 used to compute its Cartesian coordinates. Allowing n to take non-integer values defines a
 90 continuous helix in space which is close to the segmented polyline of the outer tetrahedra
 91 edges, and equals them at integer values.

92 [Figure 4](#) illustrates this difference with a 7-tetrahedra BC helix, which is in fact the same
 93 geometry as the robot illustrated in [Figure 12](#). Although the nodes coincide, [\(1\)](#) evaluated
 94 at real values generates the black helix which runs through every node, and [\(2\)](#) defines the

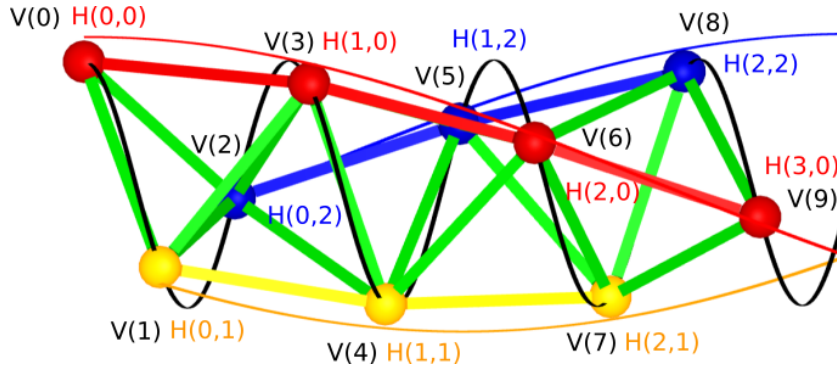


Figure 4. Rail helices (H) vs. Coxeter/Gray helix (V)

95 red, yellow, and blue helices. (In this figure these rail helices have been rendered at a slightly
96 higher radius than the nodes for clarity; in actuality the maximum distance between the
97 continuous, curved helix and the straight edges between nodes is much smaller than can be
98 clearly rendered.)

99 The quantity $(3\theta_{bc} - 2\pi) \approx 35.43^\circ$ is the angular shift between $\mathbf{V}(3n+c) = \mathbf{H}_{BCcolored}(n, c)$
100 and $\mathbf{V}(3(n+1)+c) = \mathbf{H}_{BCcolored}(n+1, c)$. This quantity appears so often that we call it the
101 “rail angle ρ ”. For the BC helix, $\rho_{bc} = (3\theta_{bc} - 2\pi)$.

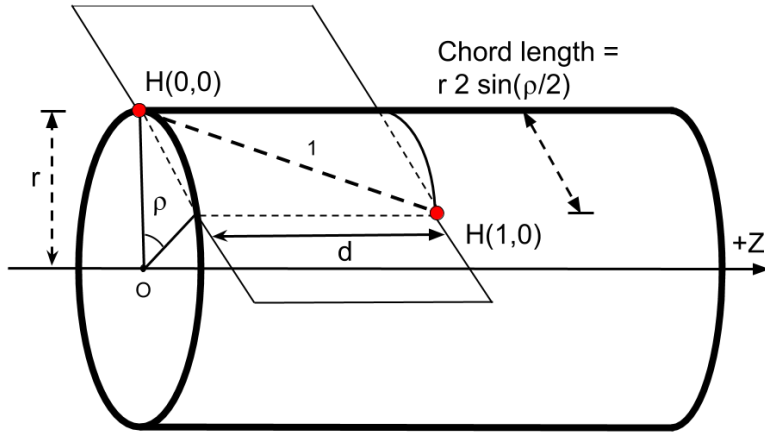


Figure 5. Rail Angle Geometry

102 Note in Figure 5 the z -axis travel for one rail edge is denoted by d . In (1) and (2),
103 the variable h is used for one third of the distance we name d . We will later justify that
104 $d = 3h$. In this paper we assume the length of a rail is always 1 as a simplification, except in

105 proofs concerning rail length. (We make the rail length a parameter in our JavaScript code
 106 in https://github.com/PubInv/tetrahelix/blob/master/js/tetrahelix_math.js [12].)

107 The $\mathbf{H}_{BC\text{colored}}(n, c)$ formulation can be further clarified by rewriting directly in terms of
 108 the rail angle ρ_{bc} rather than θ_{bc} . Intuitively we seek an expression where $c/3$ is multiplied by
 109 a $1/3$ rotation plus the rail angle ρ . We expand the expressions θ_{bc} and ρ_{bc} in (2) and seek to
 110 isolate the term $c2\pi/3$.

$$\begin{aligned} 111 \quad c\theta_{bc} &= \{\text{we aim for } 3 \text{ in denominator, so we split...}\} \\ 112 \quad (c/3)(3\theta_{bc}) &= \{\text{we want } 2\pi \text{ in numerator, so add canceling terms...}\} \\ 113 \quad (c/3)((3\theta_{bc} - 2\pi) + 2\pi) &= \{\text{definition of } \rho_{bc}\}... \\ 114 \quad (c/3)\rho_{bc} + c2\pi/3 &= \{\text{algebra...}\} \\ 115 \quad c(\rho_{bc} + 2\pi)/3 & \\ 116 \end{aligned}$$

118 This allows us to redefine:

$$119 \quad (3) \quad \mathbf{H}_{BC\text{colored}}(n, c) = \begin{bmatrix} r \cos \rho_{bc} n + c(\rho_{bc} + 2\pi)/3 \\ r \sin \rho_{bc} n + c(\rho_{bc} + 2\pi)/3 \\ (n + c/3)h_{bc} \end{bmatrix}, \text{ where } \begin{aligned} \rho_{bc} &= (3\theta_{bc} - 2\pi) \\ h_{bc} &= 1/\sqrt{10} \end{aligned}$$

120 Recall that $c \in \{0, 1, 2\}$, but n is continuous (rational or real-valued.) We can now assert
 121 that in Figure 4 the black helix winds at $\frac{3\theta_{bc}}{\rho_{bc}} \approx 11.16$ times the rate of a rail helix.

122 From this formulation it is easy to see that moving one vertex on a rail ($\mathbf{H}_{BC\text{colored}}(n, c)$)
 123 to $\mathbf{H}_{BC\text{colored}}(n + 1, c)$ for any n and c) moves us ρ_{bc} radians around a circle. Since:

$$124 \quad \frac{2\pi}{\rho_{bc}} \approx 10.16$$

125 we can see that there are approximately 10.16 red, blue or yellow tetrahedra on one rail in a
 126 single revolution.

127 The *pitch* of any tetrahelix, defined as the axial length of a complete revolution where
 128 $\rho \neq 0$ is:

$$129 \quad (4) \quad p(\rho) = \frac{2\pi \cdot d}{\rho}$$

130 The pitch of the Boerdijk-Coxeter helix of edge length 1 is the length of three tetrahedra
 131 times this number:

$$132 \quad \frac{3h_{bc} \cdot 2\pi}{\rho_{bc}} = \frac{6\pi}{\sqrt{10}\rho_{bc}} \approx 9.64$$

134 The pitch is less than the number of tetrahedra because the tetrahedra are not lined
 135 up perfectly. It is a famous and interesting result that the pitch is irrational. A BC helix
 136 never has two tetrahedra at precisely the same orientation around the z -axis. However, this

137 is inconvenient to designers, who might prefer a rational pitch. The idea of developing a
138 rational period by arranging solid tetrahedra by relaxing the face-to-face matching has been
139 explored[13]. We develop below slightly irregular edge lengths that support, for example, a
140 pitch of precisely 12 tetrahedra in one revolution which would allow an architect to design a
141 column having a basis and a capital in the same relation to the tetrahedra they touch at the
142 bottom and top of the column.

143 **3. Optimal Tetrahelices are Triple Helices.** We use the term *tetrahelix* to mean any
144 structure made of vertices and edges which is isomorphic to the BC helix and in which the
145 vertices lie on three helices. We further demand that all edge lengths be finite, as we are only
146 interested in physically constructable tetrahelices. By isomorphic we mean there is a one-
147 to-one mapping between both vertices and edges in the two tetrahelices. One could consider
148 various definitions of optimality for a tetrahelix, but the most useful to us as robotocists
149 working with the Tetrobot concept is to minimize the maximum ratio between any two edge
150 lengths, because the Tetrobot uses mechanical linear actuators with limited range of extension.

151 A *triple helix* is three congruent helices that share an axis. We show that optimal tetra-
152 helices are in fact triple helices with the same radius, so that all vertices are on a cylinder.
153 In, stages, we demonstrate that optimal tetrahelices:

- 154 1. have the same pitch,
- 155 2. have parallel axes,
- 156 3. share the same axis,
- 157 4. have the same radius,
- 158 5. have the same rail lengths,
- 159 6. have axially equidistant nodes, and therefore
- 160 7. are in fact triple helices.

161 Suppose that all three rails do not have the same pitch. Starting at any shortest edge
162 between two rails, as we move from node to node away from our start edge the edge lengths
163 between rails must always lengthen without bound, which cannot be optimal. So we are
164 justified in talking about the *pitch* of the optimal tetrahelix as the pitch of its three rail
165 helices, even though there are three such helices of equivalent pitch.

166 Similarly, if the axes are not parallel, there is an edge of unbounded length in the structure,
167 so we do not consider such cases.

168 Define a *minimax edge-length optimal tetrahelix* or just an *optimal tetrahelix* to be a
169 tetrahelix for which there exists no other tetrahelix with lower ratio of longest edge length to
170 shortest edge length.

171 We wish to show that in an optimal tetrahelix, all vertices lie on the cylinder of radius r ,
172 regardless of where they lie on the z -axis.

173 As a little lemma for the proof below, observe that a tetrahelix of zero radius, where all
174 points lie on the same line, is not as optimal as a tetrahelix of a small radius. The edges
175 between rails will be shorter than the rail edges, and moving them apart slightly lengthens
176 the between-edge rails.

177 **Theorem 1.** *Any optimal tetrahelix with a rail angle of magnitude less than π has all three
178 axes coincident.*

179 *Proof.* Case 1: Suppose that ρ is zero. Then for any given inradius, the figure in the
 180 XY -plane of an equilateral triangle is the minimax solution for all non-rail edges. Since all
 181 rail edges are of length 1, this is the minimax solution for the entire set. Since the vertices of
 182 an equilateral triangle lie on a circle, all points in three-space lie on a cylinder.

183 Case 2: Suppose that ρ is positive but less than π . In this case each rail helix has
 184 curvature. The projection of points in the XY plane creates a figure guaranteed to have
 185 point on either side of any line through the axis of such a helix, because the figure is either
 186 an n -gon or a circle. We show that the three helices share a common axis.

187 Without loss of generality define the Red helix to have its axis on the z -axis. Without
 188 loss of generativity define the Blue helix to be a helix that has an edge connection to the Red
 189 helix that is either a maximum or a minimum. Let \mathbf{B}' be the blue helix \mathbf{B} translated in the
 190 XY -plane so that its axis is the z -axis and condicent with the red helix R . Let D be the
 191 distance between the axis of the Blue helix \mathbf{B} and \mathbf{B}' . We will show that if $D > 0$ then \mathbf{B}
 192 “wobbles” in a way that cannot be optimal. Define a wobble vector by:

$$193 \quad \mathbf{W}(n) = \mathbf{B}(n) - \mathbf{B}'(n)$$

194 where $\mathbf{B}(n)$ is the cartesian vector $\begin{bmatrix} x \\ y \end{bmatrix}$ for the projection of the n th blue vertex. Note that
 195 $\|\mathbf{R}(n) - \mathbf{B}'(n + k)\|$ is a constant for any k , because R and B' have the same pitch and the
 196 same axis, even if they do not have the same radius (which we are currently proving.)

197 Figure 6 demonstrates illustrates this situation. Like most diagrams, it is over specific,
 198 in that the two circles are drawn of the same radius but we do not depend upon that in this
 199 proof. The diagram represents the projection along the z axis of points into the XY -plane.

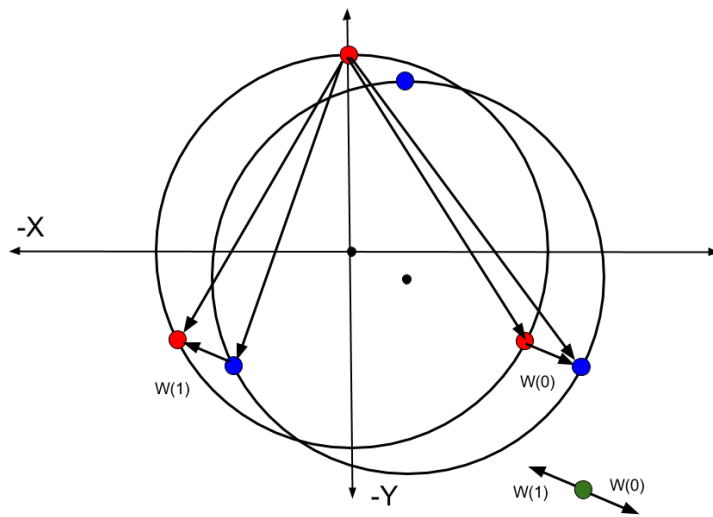


Figure 6. Wobble Vectors from Non-Coincident Axes

200 Since $-\pi < \rho < \pi$, each rail helix rotates about its axis as a function of n and defines at
 201 least 3 unique points when projected onto the XY -plane around its axis. If $2\pi/\rho$ is irrational,
 202 it defines a circle. If $2\pi/\rho$ is rational it defines an n -gon in the XY -plane, where n is at least
 203 3 (when $\rho = 2\pi/3$). The set of wobbles $\{\mathbf{W}(n)|\text{for any } n\}$ thus contains at least three vectors,
 204 pointing in different directions. For any point not at the origin, at least one of these vectors
 205 moves closer to the point and at least one moves further away.

206 The set of all lengths in the tetrahelix is a superset of: $L = \{||\mathbf{R}(n) - \mathbf{B}(n)||\}$, which by
 207 our choice has at least one longest or shortest length. $L = \{||\mathbf{R}(n) - (\mathbf{B}'(n) + \mathbf{W}(n))||\}$ and
 208 so $L = \{||(\mathbf{R}(n) - \mathbf{B}'(n)) - \mathbf{W}(n)||\}$. But $\mathbf{R}(n) - \mathbf{B}'(n)$ is a constant, so the minimax value of
 209 L is improved as $||\mathbf{W}(n)||$ decreases. By our choice, this improves the minimax value of the
 210 total tetrahelix.

211 This process can be carried out on both the Blue and Yellow helices (perhaps simulta-
 212 neously) until $\mathbf{W}(n)$ is zero for both, finding a tetrahelix of improved overall minimax value
 213 at each step. So a tetrahelix is optimal only when $\mathbf{W}(n) = 0$, and therefore when $D = 0$
 214 $\mathbf{B}(n) = \mathbf{B}'(n)$, and all three axes are conincident. ■

215 Now that we have show that axes are conincident and parallel and that the pitches are
 216 the same for all helices, we can assert that any optimum tetrahelix can be generated with an
 217 equation for helices:

218 (5)
$$\mathbf{V}_{\text{triple}}(n, c) = \begin{bmatrix} r_c \cos(n\alpha + c2\pi/3 + \phi_c) \\ r_c \sin(n\alpha + c2\pi/3 + \phi_c) \\ \frac{d(n+c/3)}{3} \end{bmatrix}, \text{where: } c \in \{0, 1, 2\}$$

219 which would not be much more complicated if the axes where not coincident. Note that we
 220 have not yet show that the relationships of the radius r or the phase ϕ for the three helies,
 221 so we denoted them with a c subscript to show they are dependent on the color. We have
 222 not yet investigated in the general case the relationships between α , r , ϕ and d in (5). In
 223 section 4 we give a more specific version of this formula which generates optimal tetrahelices.
 224 However, we observe that when $\alpha = 0$, the helices are degenerate, having curvature of 0, but
 225 because of the ϕ_c term, they are not collinear.

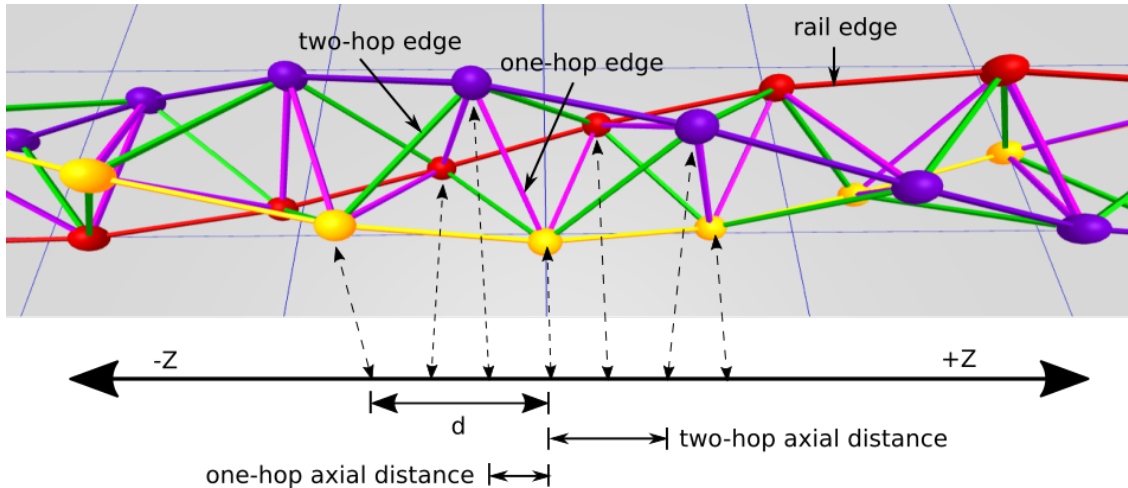


Figure 7. Edge Naming

226 In principle in any three helices generated with (5) has at most nine distinct edge length
 227 classes. Each edge that connects two rails potentially has a longer length and shorter length
 228 we denote with a + or -. So the classes are $\{RR, BB, YY, RB_+, RB_-, BY_+, BY_-, RY_+, RY_-\}$.
 229 If when projecting all vertices onto (dropping the x and y coordinates) the z -axis, the interval
 230 defined by the z axis value of its endpoints contains no other vertices, we call it a *one-hop*
 231 edge, and if it does contain another vertex we call it a *two-hop* edge, as illustrated in Figure 7.
 232 Then there are 3 rail edges $\{RR, BB, YY\}$, 3 one-hop lengths $\{RB_-, BY_-, RY_-\}$ between
 233 each pair of 3 rails, and 3 two-hop lengths $\{RB_+, BY_+, RY_+\}$ between each pair of 3 rails,
 234 where the two-hop length is at least the one-hop length. However, if we generate the three
 235 helices symmetrically with (5), many of these lengths will be the same. In fact, it is possible
 236 that there will be only two distinct such classes.

237 Now we show that an optimal tetrahelix has the same radii for all three helices. To do
 238 this we exhibit a symmetric tetrahelix (not yet shown to be optimal) which happens to be a
 239 triple helix, that has the property that all rail edges are equal to all one-hop edges and all
 240 two-hop edges are equal. Observe that although we have not yet given the formula for the
 241 radii of such a triple helix, we observe there are some values for r and α , and ϕ in (5) for which
 242 all the three helices are symmetrically and evenly spaced. Furthermore, we can choose these
 243 values such that the three rail edges are of length unity and so that the one-hop lengths are
 244 also all of length unity, and the two-hop lengths are slightly longer. We call such a tetrahelix
 245 a two-class tetrahelix.

246 Now consider a tetrahelix in which the radius of one of the helices is different. By the
 247 connections made in a tetrahelix, any increase to a radius increases both a one-hop and two-
 248 hop distance, and any decrease likewise decreases two. Since there exists a tetrahelix which
 249 has only two distinct classes of edge lengths, (the smaller being one-hop = rail, the larger
 250 being the two-hop distance), the helix with a larger radius increases a longest edge without
 251 increasing a shortest edge. Likewise, a helix with a smaller radius decreases a one-hop edge
 252 without decreasing a two-hop edge. Therefore, a tetrahelix with different radii is not as good

253 as some two-class tetrahelix generated by (5), and so it not optimal. We have not yet proved
 254 that a two-class tetrahelix is optimal, but it suffices to show that there exist such a better
 255 tetrahelix to show that different radii imply a suboptimal tetrahelix.

256 Because an optimal tetrhelix has equivalent radii and equivalent pitch for all three helices,
 257 it has equivalent rail edge lengths. Likewise, there is a single rail angle ρ that represents the
 258 rotation of two nodes connected by a single rail edge, and it is the same for all three rails.

259 Now that we have shown that any optimal tetrahelix vertices are on helices of the same
 260 axes and pitch, we see that the vertices of any optimal tetrahelix will lie on a cylinder, or a
 261 circle when axis dimension is projected out. Therefore it is reasonable to now speak of the
 262 singular *radius r* of a tetrahelix as the radius of the cylinder. We can now go on to the harder
 263 proof about where vertices occur along the z -axis.

264 We show that in fact the nodes must be distributed in even thirds along the z -axis, as in
 265 fact they are in the regular BC helix.

266 Note that from the point of view of a single edge, we are on a slanted cylinder, when
 267 $\rho \neq 0$. This means from its point of view a cross section is an ellipse. So we have to be very
 268 careful in comparing lengths of edges relative to the tetrahedron, because a change in position
 269 along the edge changes the length of a line, but in a complicated way depending on where it
 270 is relative to the ellipse.

271 However, we have already shown the rail lengths are equal in any optimal tetrahelix.

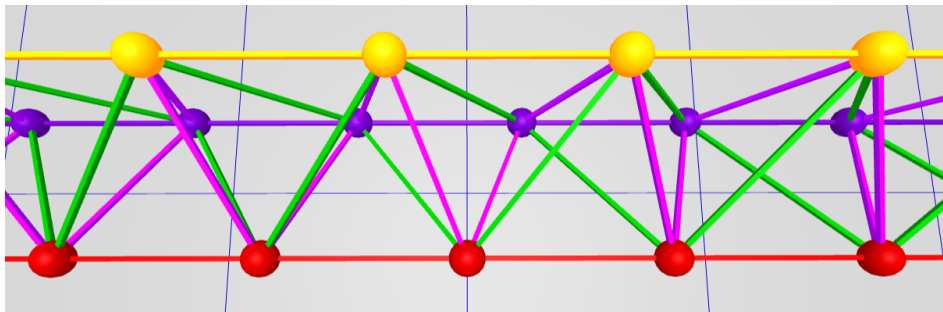


Figure 8. Equitetrabeam

272 Figure 8 shows the equitetrabeam, which is defined in [section 6](#), but also conveniently
 273 illustrates the one-hop and two-hop edge definitions. The green edges are the two-hop edges
 274 and the purple edges are the one-hop edges. Note that the green edges are slightly longer
 275 than the purple edges. In [7](#), which depicts the BC helix, the two-hop and one-hop edges are
 276 of equal length (but the projection onto the z -axis, the axial length, of the two-hop edge is
 277 longer than the axial one-hop length.)

278 **Theorem 2.** *An optimal tetrahelix of any rail angle $\rho < \pi$ is a triple helix with all vertices
 279 evenly spaced at $d/3$ intervals on the z axis. Any one tetrahedron in a tetrahelix has 1 rail
 280 edge, 2 one-hop edges connected to the rail and 2 two-hop edges connected to the rail. The
 281 edge opposite of the rail edge is a one-hop edge.*

282 **Proof.** Consider the tetrahelix in which the vertices are evenly spaced at $d/3$ intervals on
 283 the z axis. Every edge is either a rail edge, or it makes one hop, or it makes two hops. All of

284 the one-hop edges are equal length. All of the two-hop edges are equal length.

285 Every vertex is connected to 4 non-rail edges. There is a one-hop edge in both the positive
286 and negative z direction. Likewise there is a two-hop edge in both the positive and negative
287 z direction. Let A be the set of edge lengths, which has only 3 members, represented by
288 $A = \{o, t, r\}$ for the one-hop, two-hop, and rail edge lengths.

289 Any attempt to move any rail in either z direction lengthens one two-hop edge to t' , where
290 $t' > t$ and shortens one one-hop edge $o' < o$. Let $B = \{o', t'\} \cup A$ be new edges. The minimax
291 of B is greater than the minimax of A since there is a single rail length which cannot be both
292 greater than t' and o' and less than t' and o' . Therefore, any optimal tetrahelix has all one-hop
293 edges between all rails equal to each other, and all two-hop edges equal to each other, and the
294 z distances between rails equal, and therefore $d/3$ from each other. ■

295 Note that based on [Theorem 2](#), there are only 3 possible lengths in an optimal tethrahelix,
296 and we are justified in classifying edge lengths as *rail*, *one-hop*, or *two-hop*. The one-hop edges
297 are the edges between rails that are closest on the z -axis, and the two-hop edges are those
298 that skip over a vertex.

299 Taking all of these results together, each helix in an optimal tetrahelix is congruent to the
300 others, shares an axis, is the same radius, and are evenly spaced axially. An optimal tetrahelix
301 is therefore a *triple helix*.

302 **4. Parameterizing Tetrahelices via Rail Angle.** We seek a formula to generate optimal
303 tetrahelices that accepts a parameter that allows us to design the tetrahelix conveniently.
304 Please refer back to [Figure 5](#). The pitch of the helix is an obvious choice, but is not defined
305 when the curvature is 0, an important special case. The radius or the axial distance between
306 two nodes on the same rail are possible choices, but perhaps the clearest choice is to build
307 formulae that takes as their input the “rail angle” ρ . We define ρ to be the angle formed in
308 the X,Y plane $\angle \mathbf{H}(0,0)O\mathbf{H}(0,1)$ projecting out the z axis and sighting along the positive z
309 axis. In other words, ρ controls how far a rail edge of a tetrahelix deviates from being parallel
310 with the axis, or the “twistiness” of the tetrahelix. We use the parameter $\chi = 1$ to indicate a
311 chirality of counter-clockwise, and $\chi = -1$ for clockwise. We take our coordinate system to
312 be right-handed, following the convention of Three.js, our rendering software.

313 The quantities ρ, r, d are related by the expression:

$$314 \quad 1^2 = d^2 + (2r \sin \rho/2)^2 \\ 315 \quad (6) \quad d^2 = 1 - 4r^2(\sin \rho/2)^2$$

316
317 Checking the important special case of the BC helix, we find that this equation indeed
318 holds true (treating d in this equation as $3h_{bc}$ as defined by Gray and Coxeter, that is,
319 $d_{bc} = 3h_{bc}$, where they are using h for the axial height from one node to the next of a different
320 color, but we use d to mean distance between nodes of the same color).

322 The rail angle ρ also has the meaning that $2\pi/\rho$ is the number of tetrahedra in a full
323 revolution of the helix.

324 In choosing ρ , one greatly constrains r and d , but does not completely determine both of
325 them together, so we treat both as parameters.

326 Rewriting our formulation in terms of ρ :

327 (7)
$$\mathbf{H}_{general}(\chi, n, c, \rho, d_\rho, r_\rho) = \begin{bmatrix} r_\rho \cos(\chi \cdot (n\rho + c(\rho + 2\pi)/3)) \\ r_\rho \sin(\chi \cdot (n\rho + c(\rho + 2\pi)/3)) \\ d_\rho(n + c/3) \end{bmatrix}$$

328 where: $1 = d_\rho^2 + 4r_\rho^2(\sin \rho/2)^2$
 329 $\chi \in \{-1, 1\}$

330 $\mathbf{H}_{general}$ forces the user to select three values: ρ , r_ρ , and d_ρ satisfying (6).

331 Note that when $\rho = 0$ then $d_\rho = 1$, but r_ρ is not determined by (6).

332 **Theorem 3.** For rail angles of magnitude at most ρ_{bc} , tetrahelices generated by $\mathbf{H}_{general}$
 333 are optimal in terms of minimum maximum ratio of member length when radius is chosen so
 334 that the length of the one-hop edge is equal to the rail length.

335 *Proof.* This is proved by a minimax argument.

336 By Theorem 2, we can compute the (at most) three edge-lengths of an optimal tetrahelix
 337 by formula universally quantified by n and c :

338 rail = $dist(\mathbf{H}_{general}(n, c, \rho, d_\rho, r), \mathbf{H}_{general}(n+1, c, \rho, d_\rho, r)) = 1$
 339 one-hop = $dist(\mathbf{H}_{general}(n, c, \rho, d_\rho, r), \mathbf{H}_{general}(n, c+1, \rho, d_\rho, r))$
 340 two-hop = $dist(\mathbf{H}_{general}(n, c, \rho, d_\rho, r), \mathbf{H}_{general}(n, c+2, \rho, d_\rho, r))$

341

343 where $dist$ is the Cartesian distance function.

344 one-hop = $dist(\mathbf{H}_{general}(n, c, \rho, d_\rho), \mathbf{H}_{general}(n, c+1, \rho, d_\rho), r)$

345 one-hop = $\sqrt{\frac{d_\rho^2}{9} + r^2(\sin^2(\rho/3 + \frac{2\pi}{3}) + (1 - \cos(\rho/3 + \frac{2\pi}{3}))^2)}$

346 but: $d_\rho^2 = 1 - 4r^2(\sin(\rho/2)^2)$...so we substitute:

347 one-hop = $\sqrt{\frac{1}{9} + r^2(-\frac{4(\sin^2(\rho/2))}{9} + \sin^2(\rho/3 + \frac{2\pi}{3}) + (1 - \cos(\rho/3 + \frac{2\pi}{3}))^2)}$

348

350 By similar algebra and trigonometry:

351 two-hop = $\sqrt{\frac{4}{9} + r^2(-\frac{16(\sin^2(\rho/2))}{9} + \sin^2(2\rho/3 + \frac{4\pi}{3}) + (1 - \cos(2\rho/3 + \frac{4\pi}{3}))^2)}$

352

354 By definition of minimax edge length optimality, we are trying to minimize:

355
$$\frac{\max \{1, \text{one-hop}(r), \text{two-hop}(r)\}}{\min \{1, \text{one-hop}(r), \text{two-hop}(r)\}}$$

356 But since $\text{two-hop}(r) \geq \text{one-hop}(r)$, this is equivalent to:

357

$$\frac{\max\{1, \text{two-hop}(r)\}}{\min\{1, \text{one-hop}(r)\}}$$

358 This quantity will be equal to one of:

359 (8)
$$\frac{\text{two-hop}(r)}{1}, \frac{1}{\text{one-hop}(r)}, \frac{\text{two-hop}(r)}{\text{one-hop}(r)}$$

360 We know that both $\text{one-hop}(r)$ and $\text{two-hop}(r)$ increase monotonically and continuously
361 with increasing r . By inspection it seems likely that we will minimize this set by equating
362 $\text{one-hop}(r)$ or $\text{two-hop}(r)$ to 1, but to be absolutely sure and to decide which one, we must
363 examine the partial derivative of the ratio $\frac{\text{two-hop}(r)}{\text{one-hop}(r)}$ in this range.

364 Although complicated, we can use Mathematica to investigate the partial derivative of the
365 $\text{two-hop}(r) - \text{one-hop}(r)$ with respect to the radius to be able to understand how to choose
366 the radius to form the minimax optimum.

367 Let:

368

$$f_\rho = -\frac{4(\sin^2(\rho/2))}{9}$$

369

370

$$g_\rho = -\frac{16(\sin^2(\rho/2))}{9}$$

371

$$j_\rho = \sin^2(\rho/3 + \frac{2\pi}{3}) + (1 - \cos(\rho/3 + \frac{2\pi}{3}))^2$$

372

373

$$k_\rho = (\sin^2(2\rho/3 + \frac{4\pi}{3}) + (1 - \cos(2\rho/3 + \frac{4\pi}{3}))^2)$$

374 Then:

375

$$\frac{\text{two-hop}(r_\rho)}{\text{one-hop}(r_\rho)} = \frac{\sqrt{\frac{4}{9} + r^2(g_\rho + j_\rho)}}{\sqrt{\frac{1}{9} + r^2(f_\rho + k_\rho)}}$$

376

377 By graph inspection using Mathematica (<https://github.com/PubInv/tetrahelix/blob/master/tetrahelix.nb>), we see the partial derivative of this with respect to radius r is always
378 negative, for any $\rho \leq \rho_{bc}$. (When the rail angle approaches π , corresponding to going almost to
379 the other side of the tetrahelix, this is not necessarily true, hence the limitation in our state-
380 ment of the theorem is meaningful.) Since the partial derivative of $\text{two-hop}(r)/\text{one-hop}(r)$
381 with respect to the radius r is negative for all ρ up until ρ_{bc} , this ratio goes down as the radius
382 goes up, and we minimize the maximum edge-length ratio by choosing the largest radius up
383 until $\text{one-hop} = 1$, the rail-edge length. If we attempted to increase the radius further we

385 would not be optimal, because the ratio $\frac{\text{two-hop}(r)}{1}$ would be because the largest ratio in our set
 386 of ratios (8).

387 Therefore we decrease the minimax length of the whole system as we increase the radius
 388 up to the point that the shorter, one-hop distance is equal to the rail-length, 1. Therefore, to
 389 optimize the whole system so long as $\rho \leq \rho_{bc}$, we equate one-hop to 1 to find the optimum
 390 radius:

$$391 \quad 1 = \sqrt{\frac{1}{9} + r_{opt}^2 \left(-\frac{4(\sin^2(\rho/2))}{9} + \sin^2(\rho/3 + \frac{2\pi}{3}) + (1 - \cos(\rho/3 + \frac{2\pi}{3}))^2 \right)}$$

$$392 \quad (9) \quad r_{opt} = \frac{2}{\sqrt{\frac{9}{2} \cdot (\sqrt{3}\sin(\rho/3) + \cos(\rho/3)) + \cos(\rho) + 8}}$$

393

395 We can now give a formula for d_{opt} computed from ρ, r_{opt} via the rail angle equation (6):

$$396 \quad d_{opt}^2 = 1 - 4 \left(\frac{2}{\sqrt{\frac{9}{2} \cdot (\sqrt{3}\sin(\rho/3) + \cos(\rho/3)) + \cos(\rho) + 8}} \right)^2 (\sin \rho/2)^2$$

$$397 \quad d_{opt}^2 = 1 - \frac{16(\sin \rho/2)^2}{9(\sqrt{3}\sin(\rho/3) + \cos(\rho/3)) + \cos(\rho) + 8}$$

$$398 \quad (10) \quad d_{opt} = \sqrt{1 - \frac{16 \sin^2(\rho/2)}{\cos(\rho) + 9(\sqrt{3}\sin(\rho/3) + \cos(\rho/3)) + 8}}$$

399

401 Thus, by computing r_{opt} and d_{opt} as a function of ρ from this equation, we can construct
 402 minimax optimal tetrahelix for an $0 \leq \rho \leq \rho_{bc}$. ■

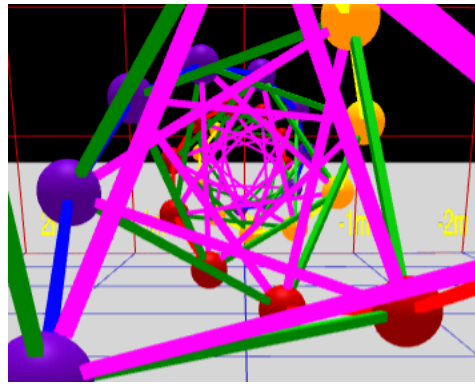


Figure 9. Axial view of a BC-Helix

403 **5. The Inradius.** Since the axes are parallel, we may define the *inradius*, represented by
 404 the letter i , of a tetrahelix to be the radius of the largest cylinder parallel to this axis that is

405 surrounded by each tetrahelix and pentrated by no edge.

406 If we look down the axis of an optimal tetrahelix as shown in [Figure 9](#), it happens that
 407 only the one-hop edges (rendered in purple in our software) comes closest to the axis. In other
 408 words, they define the radius of the incircle of the projection, or the radius of a cylinder that
 409 would just fit inside the tetrahelix. A formula for the inradius of the tetrahelix is useful if
 410 you are designing it as a structure that bears something internally, such as a firehose, a pipe,
 411 or a ladder for a human. The inradius $r_{in}(\rho)$ of an optimal tetrahelix is a remarkably simple
 412 function of the radius r and the rail angle ρ :

413 (11)
$$r_{in}(\rho) = r \sin \frac{\pi - \rho}{6}$$

414 Which can be seen from the trigonometry of a diagram of the projected one-hop edges con-
 415 necting four sequentially numbered vertices:

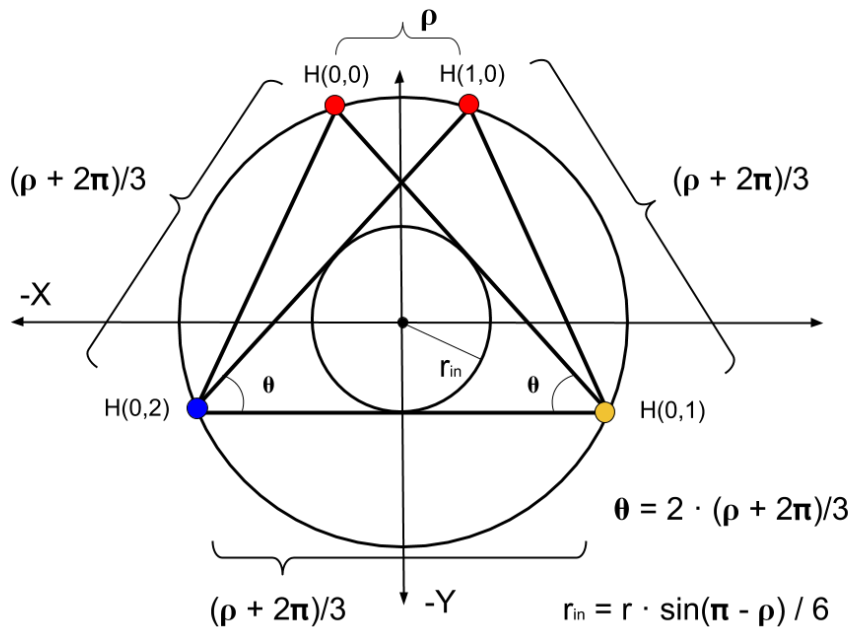


Figure 10. General One-hop Projection Diagram

416 From this equation with the help of symbolic computation we observe that inradius of the
 417 BC helix of unit rail length is $r_{in}(\rho_{bc}) = \frac{3}{10\sqrt{2}} \approx 0.21$.

418 **6. The Equitetrabeam.** Just as $\mathbf{H}_{general}$ constructs the BC helix (with careful and non-
 419 obvious choices of parameters) which is an important special case due to its regularity, it
 420 constructs an additional special (degenerate) case when the rail angle $\rho = 0$ and $d = 1$ (the
 421 edgelength), where the cross sectional area is an equilateral triangle of unchanging orientation,
 422 as shown in [Figure 8](#) and at the rear of [Figure 3](#). We call this the *equitetrabeam*. It is not

423 possible to generate an equitetrabeam from (1) without the split into three rails introduced
 424 by (2) and completed in (7).

425 **Corollary 4.** *The equitetrabeam with minimal maximal edge ratio is produced
 426 by $\mathbf{H}_{\text{general}}$ when $r = \sqrt{\frac{8}{27}}$.*

427 *Proof.* Choosing $d = 1$ and $\rho = 0$ we use Equation (9) to find the radius of optimal
 428 minimax difference.

429 Substituting into (7):

$$430 \quad \text{one-hop} = \sqrt{\frac{1}{9} + 3r^2}$$

431

433 Then:

$$434 \quad 1 = \sqrt{\frac{1}{9} + 3r^2} \quad \text{solved by...}$$

$$435 \quad r = \sqrt{\frac{8}{27}} \quad \approx 0.54$$

436

■

438 This radius¹ produces a two-hop rail length of $\frac{2}{\sqrt{3}}$. The difference between this and 1 is
 439 $\approx 15.47\%$. The inradius of the equitetrabeam of unit rail length from both Equation (11) and
 440 the fact that the inradius of an equilateral triangle is half the circumradius is $\sqrt{\frac{8}{27}}/2$, or $\frac{\sqrt{6}}{9}$.

441 In Figure 3, the furthest tetrahelix is the optimal equitetrabeam. Figure 8 is a closeup of
 442 an equitetrabeam.

443 To the extent that we value tetrabeams (that is, tetrahelices with a rail angle of 0, and
 444 therefore zero curvature and curvature) as mathematical or engineering objects, we have
 445 motivated the development of $\mathbf{H}_{\text{general}}$ as a transformation of $\mathbf{V}(n)$ defined by Equation (1)
 446 from Gray and Coxeter. It is difficult to see how the $\mathbf{V}(n)$ formulation could ever give rise
 447 to a continuum producing the tetrabeam, since setting the angle in that equation to zero can
 448 produce only collinear points.

449 The equitetrabeam may possibly be a novel construction. The fact that 6 members meet
 450 in a single point would have been a manufacturing disadvantage that may have dissuaded
 451 structural engineers from using this geometry. However, the advent of additive manufacturing,
 452 such a 3D printing, and the invention of two distinct concentric multimember joints[15, 7] has
 453 improved that situation.

454 Note that the equitetrabeam has chirality, which becomes important in our attempt to
 455 build a continuum of tetrahelices.

¹Another interesting but non-optimal solution is derived by setting $(\text{one-hop} + \text{two-hop})/2 = 1$, occurs at $r = \sqrt{35}/4$ which produces three length classes of $11/12, 12/12, 13/12$.

456 **7. An Untwisted Continuum.** We observe that Equations (9) and (10) compute r_{opt}
 457 and d_{opt} which create an optimal tetrahelix for any rail angle ρ between 0, which gives the
 458 equitetrabeam and $\rho_{bc} \approx 35.43^\circ$, which gives the BC helix.

459 Because the equitetrabeam which has a rail angle of 0 still has chirality, that is, one still
 460 must decide to connect the one-hop edge to the clockwise or the counter-clockwise node, it is
 461 not possible to build a smooth continuum where ρ transitions from positive to negative which
 462 remains optimal. One can use a negative ρ in $\mathbf{H}_{general}$ but it does not produce minimax
 463 optimal tetrahelices. In other words, untwisting a counter-clockwise tetrahelix to rail angle 0
 464 and then going even further does produce a clockwise tetrahelix, but one in which the one-hop
 465 and two-hop lengths in the wrong places (that is, two-hop becomes shorter than one-hop.)
 466 Likewise, $\rho > \rho_{bc}$ generates a tetrahelix, but minimax optimality is not guaranteed by $\mathbf{H}_{general}$.

467 The pitch of a helix (see (4), for a fixed z -axis travel d , is trivial. However, if one is
 468 computing z -axis travel from (10) the pitch is not simple. It increases monotonically and
 469 smoothly with decreasing ρ , so Equation (4) can be easily solved numerically with a Newton-
 470 Raphson solver, as we do on our website. For a pitch at least $p \geq \frac{3\sqrt{2}\pi}{\sqrt{5}\rho_{bc}} \approx 9.64$, using (10)
 471 produces minimax optimal tetrahelices.

472 In this way a rail angle can be chosen for any desired (sufficiently large) pitch, yield the
 473 optimum radius, one-hop, and two-hop lengths an engineer needs to construct a physical
 474 structure.

475 The curvature of a rail helix is formally given by:

476 (12)
$$\frac{|r_\rho|}{r_\rho^2 + (d_\rho/\rho)^2}$$

477 which goes to 0 as ρ approaches 0 (the equitetrabeam.) As ρ increase up to ρ_{bc} the curvature
 478 increases smoothly until the BC Helix is reached.

479 Perhaps surprisingly, the optimal untwisting is accomplished only by changing the length
 480 of the two-hop member, leaving the one-hop member and rail length equivalent within this
 481 continuum.² However, it should be noted that an engineer or architect may also use $\mathbf{H}_{general}$
 482 directly and interactively, and that minimax length optimality is a mathematical starting point
 483 rather than the final word on the beauty and utility of physical structures. For example, a
 484 structural engineer might increase radius past optimality in order to resist buckling.

485 If an equitetrabeam were actually used as a beam, an engineer might start with the
 486 optimal tetrabeam and dilate it in one dimension to “deepen” the beam. Similarly, simple
 487 length changes curve the equitetrabeam into an “arch”. The “colored” approach of (7) exposes
 488 these possibilities more than the approach of (1).

489 Trusses and space frames remain an important design field in mechanical and structural
 490 engineering[10], including deployable and moving trusses[2].

²Before deriving Equation (9), we created a continuum by using a linear interpolation between the optimal radius for the Equitetrabeam and the BC Helix. This minimax optimum of this simpler approach was at most 1% worse than the optimum computed by (9).

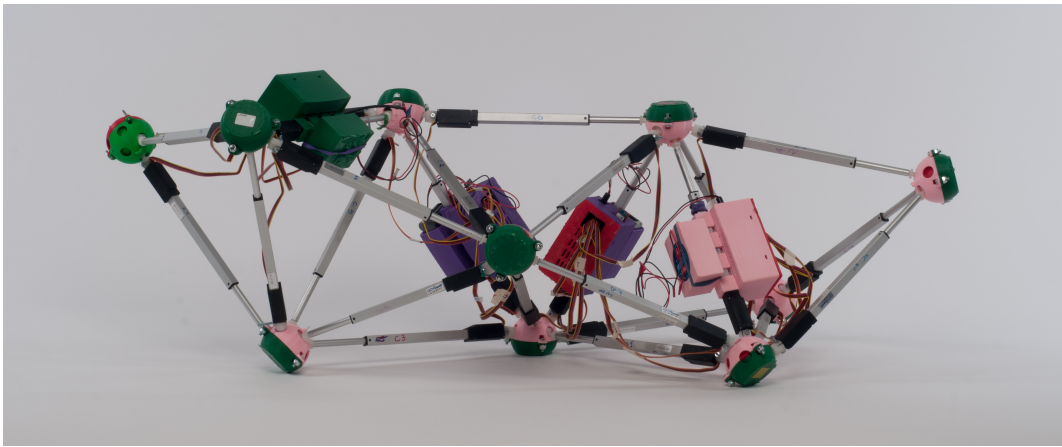


Figure 11. *Glussbot in relaxed, or BC helix configuration*

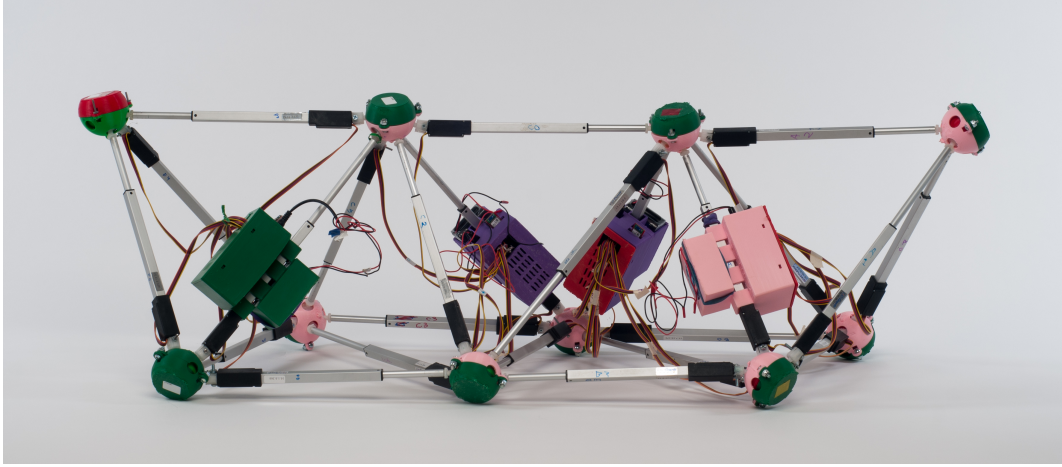


Figure 12. *The Equitetrabream: Fully Untwisted Glussbot in Hexapod Configuration*

491 **8. Utility for Robotics.** Starting twenty years ago, Sanderson[14], Hamlin,[8], Lee[9], and
 492 others created a style of robotics based on changing the lengths of members joined at the
 493 center of a joint, thereby creating a connection to pure geometry. More recently NASA has
 494 experimented with tensegrities[1], a different point in the same design spectrum. These fields
 495 create a need to explore the notion of geometries changing over time, not generally considered
 496 directly by pure geometry.

497 As suggested by Buckminster Fuller, the most convenient geometries to consider are those
 498 that have regular member lengths, in order to facilitate the inexpensive manufacture and
 499 construction of the robot. In a plane, the octet truss[4] is such a geometry, but in a line, the
 500 Boerdijk-Coxeter helix is a regular structure.

501 However, a robot must move, and so it is interesting to consider the transmutations of
 502 these geometries, which was in fact the motivation for creating the equitetrabream.

503 **Theorem 5.** *By changing only the length of the longer members that connect two distinct
 504 rails (the two-hop members), we can dynamically untwist a tetrobot forming the Boerdijk-*

505 Coxeter configuration into the equitetrabeam which rests flat on the plane.

506 *Proof.* Proof by our computer program that does this using Equation (7) applied to the
507 7-tet Tetrobot/Glussbot.

508 By untwisting the tetrahelix so that it has a planar surface resting on the ground, we may
509 consider each vertex touching the ground a foot or pseudopod. A robot can thus become a
510 hexapod or n -pod robot, and the already well-developed approaches to hexapod gaits may be
511 applied to make the robot walk or crawl.

512 **9. Conclusion.** The BC Helix is the end point of a continuum of tetrahelices, the other end
513 point being an untwisted tetrahelix with equilateral cross section, constructed by changing the
514 length of only those members crossing the outside rails after hopping over the nearest vertex.
515 Under the condition of minimum maximum length ratios of all members in the system, all
516 such tetrahelices have vertices evenly spaced along the axis generated by a simple equation
517 and are in fact triple helices. A machine, such as a robot or a variable-geometry truss, that
518 can change the length of its members can thus twist and untwist itself by changing the length
519 of the appropriate members to achieve any point in the continuum. With a numeric solution,
520 a design may choose a rotation angle and member lengths to obtain a desired pitch.

521 **10. Contact and Getting Involved.** The Gluss Project <http://pubinv.github.io/gluss/> is
522 part of Public Invention <https://pubinv.github.io/PubInv/>, a free-libre, open-source research,
523 hardware, and software project that welcomes volunteers. It is our goal to organize projects for
524 the benefit of all humanity without seeking profit or intellectual property. To assist, contact
525 read.robert@gmail.com.

526

REFERENCES

- 527 [1] *NTRT - NASA Tensegrity Robotics Toolkit.* <https://ti.arc.nasa.gov/tech/asr/intelligent-robotics/tensegrity/ntrt/>. Accessed: 2016-09-13.
- 528 [2] J. CLAYPOOL, *Readily configured and reconfigured structural trusses based on tetrahedrons as modules*,
529 Sept. 18 2012, <https://www.google.com/patents/US8266864>. US Patent 8,266,864.
- 530 [3] H. COXETER ET AL., *The simplicial helix and the equation $\tan(n \theta) = n \tan(\theta)$* , Canad. Math. Bull, 28
531 (1985), pp. 385–393.
- 532 [4] R. FULLER, *Synergetic building construction*, May 30 1961, <https://www.google.com/patents/US2986241>.
533 US Patent 2,986,241.
- 534 [5] R. FULLER AND E. APPLEWHITE, *Synergetics: explorations in the geometry of thinking*, Macmillan, 1982,
535 <https://books.google.com/books?id=G8baAAAAMAAJ>.
- 536 [6] R. W. GRAY, *Tetrahelix data*. <http://www.rwgrayprojects.com/rbfnotes/helix/helix01.html>, <http://www.rwgrayprojects.com/rbfnotes/helix/helix01.html> (accessed Accessed: 2017-04-08).
- 537 [7] G. J. HAMLIN AND A. C. SANDERSON, *A novel concentric multilink spherical joint with parallel robotics*
538 *applications*, in Proceedings of the 1994 IEEE International Conference on Robotics and Automation,
539 May 1994, pp. 1267–1272 vol.2, <https://doi.org/10.1109/ROBOT.1994.351313>.
- 540 [8] G. J. HAMLIN AND A. C. SANDERSON, *Tetrobot: A Modular Approach to Reconfigurable Parallel*
541 *Robotics*, Springer Science & Business Media, 2013, <https://play.google.com/store/books/details?id=izrSBwAAQBAJ> (accessed 2017-04-08).
- 542 [9] W. H. LEE AND A. C. SANDERSON, *Dynamic rolling locomotion and control of modular robots*, IEEE
543 Transactions on robotics and automation, 18 (2002), pp. 32–41.
- 544 [10] M. MIKULAS AND R. CRAWFORD, *Sequentially deployable maneuverable tetrahedral beam*, Dec. 10 1985,
545 <https://www.google.com/patents/US4557097>. US Patent 4,557,097.

- 549 [11] R. L. READ, *Gluss = Slug + Truss*. Unpublished preprint, <https://github.com/PubInv/gluss/blob/gh-pages/doc/Gluss.pdf> (accessed 2016-10-27).
- 550 [12] R. L. READ, *Untwisting the tetrahelix website*. <https://pubinv.github.io/tetrahelix/>, <https://pubinv.github.io/tetrahelix/> (accessed 2017-04-08).
- 551 [13] G. SADLER, F. FANG, J. KOVACS, AND K. IRWIN, *Periodic modification of the Boerdijk-Coxeter helix (tetrahelix)*, arXiv preprint arXiv:1302.1174, (2013), <https://arxiv.org/abs/1302.1174>.
- 552 [14] A. C. SANDERSON, *Modular robotics: Design and examples*, in Emerging Technologies and Factory Au-
553 tomation, 1996. EFTA'96. Proceedings., 1996 IEEE Conference on, vol. 2, IEEE, 1996, pp. 460–466.
- 554 [15] S. SONG, D. KWON, AND W. KIM, *Spherical joint for coupling three or more links together at one point*,
555 May 27 2003, <http://www.google.com/patents/US6568871>. US Patent 6,568,871.
- 556
- 557
- 558